SSC25-RAVIII-06

Augmenting Attitude Knowledge for Optical Communication Terminals on CubeSats by Kalman Filter Based Estimation

Elisa Garbagnati, René Rüddenklau, Christopher Schmidt
Institute of Communications and Navigation, German Aerospace Center (DLR)
Münchener Straße 20, Weßling, 82234, Germany; +498153284920
elisa.garbagnati@dlr.de

ABSTRACT

Given the growing demand for high data rate transmission on small satellites like CubeSats, free-space optical communication terminals have recently attracted an increasing interest thanks to their capability of ensuring high data rates, compact designs and low power requirements. Yet, the performances of the acquisition and pointing processes crucially depend on their attitude knowledge information. This information is currently available only if an optical link has already been established. Nevertheless, it is likewise important to accurately know the attitude during the link acquisition phase to shorten the search time until the opposing target is found. This aspect is equally relevant in the context of Inter-Satellite Links between CubeSats and for enhancing Direct-To-Earth communications.
Indeed, this work presents an attitude estimation concept for CubeSats housing Laser Communication Terminals (LCT), aiming to augment the system's attitude knowledge to establish optical links and maintain them over time.
Linear extrapolation and quaternion kinematics propagation have been initially investigated for a basic estimation relying on the CubeSat's ADCS telemetry. Hence a more sophisticated algorithm has been developed consisting of a USQUE Unscented Kalman Filter according to the model of Crassidis and Markley, 2003. This proposed algorithm relies on the attitude information given by the CubeSat's ADCS as well as on the measurements coming from the LCT's sensors. A comparative analysis between the algorithms has been undertaken for a dynamic and a stable scenarios in terms of pointing accuracy to investigate the improvement achieved by exploiting the Kalman filter and the information of the LCT.
From simulations, the Kalman filter-based estimation algorithms proved to grant a fast convergence and an accurate estimation of the CubeSat's attitude. Thanks to this augmented knowledge that relies on the LCT information, it is hence possible to shorten the search time needed to establish an optical link and to easily compensate for pointing errors during the tracking phase of the mission.

INTRODUCTION

Satellites play an important role in almost every part of our daily lives and with this, the role and size of satellites changed over the past years. Small satellites are used for communication, gathering data from our atmosphere, Earth observation and many more. With this, also the requirements for communication volumes grew and especially on small satellites with limited resources, optical communication can help to overcome the bottleneck in communication between the satellites and from the satellite to ground.[1] While the high data rate of optical communication is obvious, it comes for the prize of small beam divergences - allowing for a higher power density on the receiver side but introducing challenges on the pointing of the narrow laser beam. In Direct-to-Earth (DTE) scenarios, a large Optical Ground Station (OGS) with a comparably large divergence of the beacon system is assumed, as well as a precise orbit knowledge of the satellite to ensure that satellite gets illuminated from the OGS's beacon system. To establish a link between the laser terminal onboard the satellite and the OGS, the laser terminal scans for the OGS's beacon - with increased attitude knowledge, reducing the scan area and therefore also the time until the link is used for data transmission.[2,3]
In contrast to the DTE scenario, optical Inter-Satellite Links (ISL) can't rely on a OGS with high laser power and large divergence. The two laser terminals onboard the satellites need to establish a link and therefore use an algorithm for scanning on both sides - with small divergences, the time for acquiring the signal grows exponentially with the inaccuracy of the attitude knowledge between the terminals.[4]
Therefore, in this work a concept to increase the attitude knowledge available to the Laser Communica-

tion Terminal (LCT) is presented in order to shorten the link acquisition phase. The proposed concept combines the attitude data of the satellite's Attitude Dynamics and Control System (ADCS) and the LCT's sensors measurements to augment the attitude knowledge during pointing without optical feedback through the use of Kalman filter estimations. This method is here addressed to the scenario of CubeISL, a mission developed by the German Aerospace Center (DLR) to demonstrate optical downlinks up to 1 Gbps and exchange of operational data via bidirectional optical links up to 100 Mbps between two LCTs on-board of two 6U CubeSats.[5] In detail, the CubeSat platforms are assumed to reach an attitude knowledge of ± 0.1 deg while the considered LCT can compensate for satellite pointing errors up to 1 deg. Indeed, the goal of this work is to provide an augmented satellite attitude information to the LCT to allow it to compensate for bigger errors in a feed-forward manner.

CUBEISL DIRECT-TO-EARTH AND INTER-SATELLITE LINK SCENARIOS

Establishing optical links between two LCTs on 6U CubeSats demands precise attitude control due to the narrow laser beam divergence. This section evaluates current CubeSat platforms to understand the challenges in achieving and maintaining such links. A 6U CubeSat is used as a baseline to analyze performance under realistic disturbances and explore mitigation strategies like propagation algorithms and attitude data exchange. Relevant disturbances include micro-vibrations and pointing instability arising from limited control accuracy between ADCS updates.

CubeISL Mission Overview

The CubeISL payload is structured into three modular components: the optical amplifier, the optical block, and the data/interface module. This modular design enables parallel development and integration. The system is compact, fitting within the 1U CubeSat standard. Each module plays a distinct role in signal amplification, data handling, and optical communication. The payload includes an Fine Pointing Assembly (FPA) to ensure precise beam alignment and efficient data transfer, with built-in mechanisms to maintain performance and reliability over time. The FPA consists mainly of a 4-Quadrant Diode (4QD) to acquire the beacon and measure the angular offset, a Fast Steering Mirror (FSM) to correct the measured error and a Microcontroller (µC) to process the control loop.[5]

The payload will be employed in the CubeISL mission, aiming to demonstrate high data-rates DTE and ISL communication between two identical 6U CubeSats flying in a trailing constellation in the Low Earth Orbit (LEO) region (Figure 1). The terminals are referred as CubeISL(A) and CubeISL(B) and emit/receive signals at opposite wavelengths: terminal (A) emits at 1537 nm and receives at 1553 nm, while (B) emits at 1553 nm and receives at 1537 nm. Both can then receive light at 1590 nm from the OGSs and perform downlinks up to 1 Gbps. The proposed mission concept accounts for the two launched ISL terminals and two OGSs to demonstrate interoperability between the ground stations: a possible use case consists in an optical uplink from a first OGS to terminal (A), an optical ISL between the terminals and a downlink from terminal (B) to a second OGS as presented below.

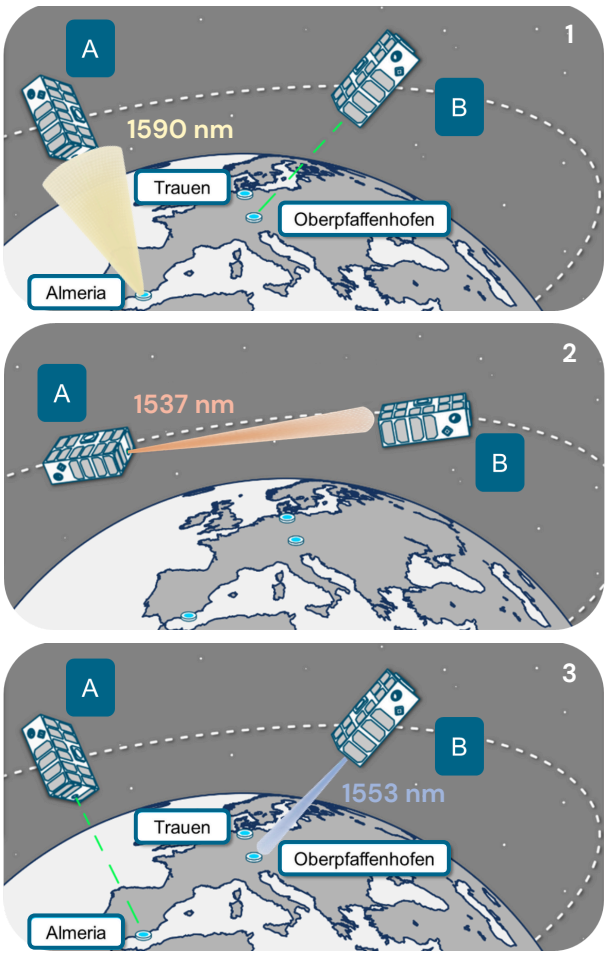

Figure 1: CubeISL mission concept for Direct-To-Earth Communication with the OGSs (1 and 3) and Inter-Satellite Links between the two terminals (2).

A key challenge in Inter-Satellite Links is the acquisition process, which is more complex than for DTE due to narrower beams and lower power on-orbit. CubeISL addresses this with an asymmetric, unsynchronized acquisition scheme where each terminal follows a tailored search pattern. Terminals operate as either T-PAT (terminal for pointing, acquisition and tracking) or T-DAT (terminal for detection, adjusting and tracking), detecting signal hits and adjusting pointing accordingly. The process transitions to tracking mode based on signal detection and timing, with safeguards to prevent false lock-in. This design allows both terminals to be interchangeable via software, simplifying operation within satellite constellations.[6]

Attitude Estimation Concept

Traditional CubeSat platforms consist of separate subsystems that operate independently. The proposed concept enhances performance by enabling information exchange between subsystems, particularly the ADCS and the LCT (Figure 2).[3] Since LCTs require faster control updates than typical ADCS systems, a dedicated estimation algorithm is introduced for the LCT, initialized with ADCS data and refined using onboard sensors like micro-electromechanical system (MEMS) gyroscopes and magnetometers. This approach aims to improve attitude knowledge between ADCS updates and can be extended to other high-rate sensors, provided proper calibration is performed.

As depicted, the precise estimated attitude is sampled by the satellite and forwarded at 1 Hz to the LCT. The LCT uses this data and propagates it at a higher sampling frequency with its less precise onboard sensors. This ensures that the propagation of the ADCS data covers also dynamic changes in attitude which would not be covered by linear extrapolation. The retrieved attitude is then compared with the pointing target vector and finally the pointing error is calculated. Since the pointing error is now known, the FSM can be used to compensate it in a feed-forward manner. Therefore the LCT is able to compensate the less accurate actuators of the satellite by employing its precise fine pointing assembly. During the acquisition phase, this higher accuracy in the attitude knowledge results in a shorter search-time for the link establishment.

Once the link is established, indeed, the FSM changes its reference source from the estimated attitude to the measured relative error provided by the 4-quadrant diode. In future developments, this latter measured error could then be given as an attitude feedback input to the satellite's ADCS to further improve its pointing and link stability during the tracking phase of the mission[3] (indicated by dashed red lines in Figure 2).

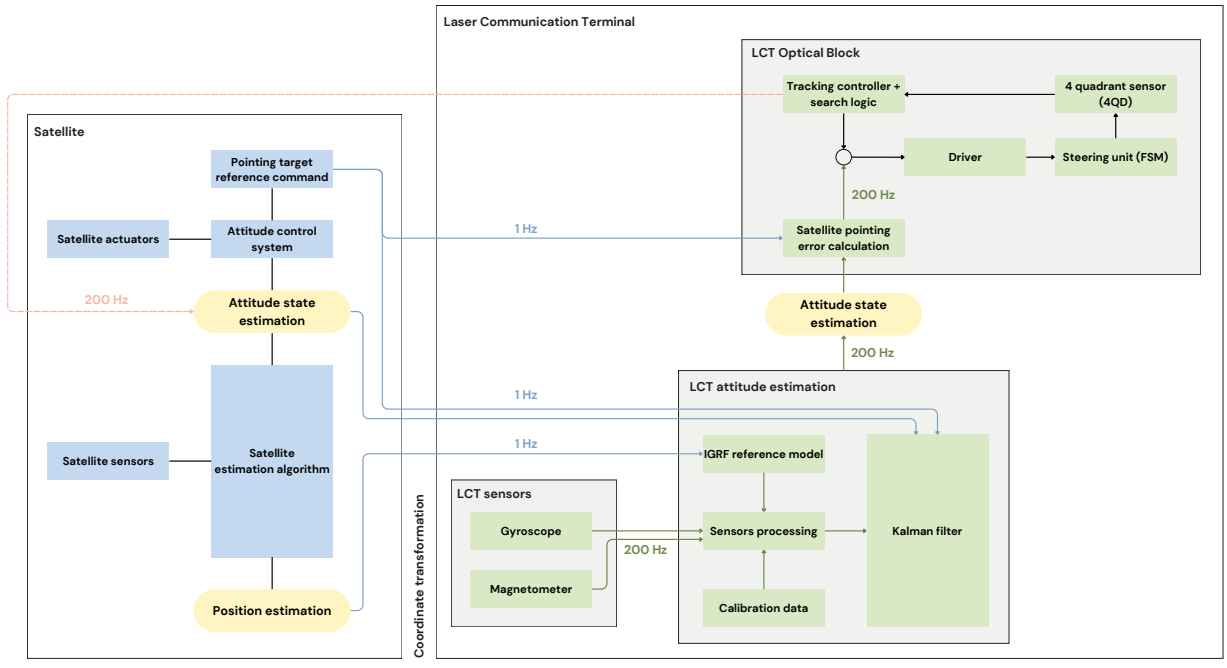

Figure 2: Proposed attitude estimation concept based on a gyroscope and a magnetometer as LCT's sensors and a data interface between the LCT and the satellite ADCS subsystem.

SATELLITE AND LCT MODELS

As introduced in the estimation concept, the proposed attitude estimation relies on the information provided by the satellite ADCS and the optical communication terminal. Therefore, the models of the CubeISL's satellite ADCS and the LCT have been implemented in the SIMULINK environment to simulate the satellite's attitude and study the attitude estimation of the LCT.
With regard to this work, the satellite body frame is indicated with the subscript B, the fixed inertial ECI frame (Earth-Centered Inertial) is indicated with the subscript N and the LVLH (local-vertical local-horizontal) one is indicated by L. The LCT is then considered to be positioned on the side of the CubeSat: the origins of the satellite and LCT frames are arbitrarily set respectively in the center of mass of the 6U CubeSat body and in the geometric center of the lateral face for the LCT (Figure 3).

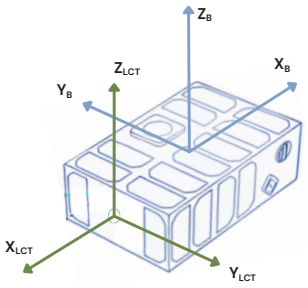

Figure 3: Reference frames for the satellite body (blue) and the LCT optical block (green) for the CubeISL payload.

The resulting coordinates transformation for the attitude quantities between the reference frames is therefore represented by the rotation matrix in Equation 1, while no additional translation is considered for transforming angular quantities.

$$R_{\mathrm{LCT}\leftarrow\mathrm{B}} = R_{\mathrm{B}\leftarrow\mathrm{LCT}} = \begin{bmatrix} -1 & 0 & 0 \\ 0 & -1 & 0 \\ 0 & 0 & 1 \end{bmatrix} \tag{1}$$

CubeISL's ADCS baseline

The baseline model of the CubeISL's ADCS consists of a 6U CubeSat in a LEO orbit featuring an ADCS closed-loop control. The loop is assumed to work at 1 Hz, according to conventional ADCS. Its aim is to simulate a plausible real-time behavior of the CubeSat's attitude quantities - quaternions $\boldsymbol{q}_{\mathrm{ADCS}}$ and angular velocity $\boldsymbol{\omega}_{\mathrm{ADCS}}$ - that can then be fed to the LCT. The model's block diagram is shown in Figure 4. The CubeSat's physical representation includes modeling of orbital motion, space environment and disturbances, dynamics and kinematics, sensors, actuators and desired attitude. The satellite software includes determination and control algorithms and filters.

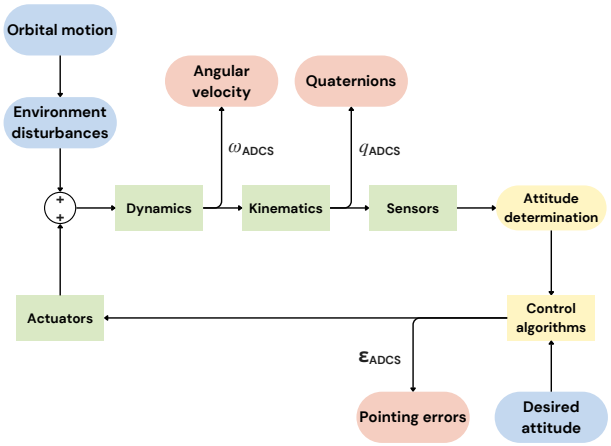

Figure 4: ADCS closed-loop control of the CubeISL baseline model.

The satellite bus is assumed to be a 6-Unit CubeSat with an assumed total mass of 8 Kg and is modeled as a parallelepiped of dimensions 0.1 m×0.2 m×0.3 m with uniformly distributed mass (Figure 3). No appendages have been here considered, except for two 1U × 2U solar panels considered as not-deployed and lying along the X−Z surfaces of the CubeSat. Moreover, the CubeSat is assumed to be equipped with the following components, modeled and positioned according to a proposed disposition:[7]

- Sensors: a sun sensor, a magnetometer, a horizon sensor, a gyroscope, a star tracker (positioned along $\mathrm{Y_B}$).
- Actuators: a set of 3 magnetorquers (along the three principal axes), a set of 4 reaction wheels (in a pyramidal configuration)

The CubeISL orbit is here defined as a circular LEO orbit with an altitude of 522.17 km, compliant with the CubeISL mission's altitude requirements.[4] On this orbital path, the satellite is assumed to be subject to several environmental disturbances, which have been implemented as external torques in the principal inertia axes reference frame:[7] the main contributors considered are the gravity gradient, the solar radiation pressure, the aerodynamic drag and the magnetic field.
The dynamics of the CubeSat is governed by Euler's equations[8] which consist of a system of non-linear differential equations. Integrating the Euler equations yields to find the angular velocity vector of the spacecraft $\boldsymbol{\omega} = \boldsymbol{\omega}_{\mathrm{ADCS}}$.

From the angular velocity, it is possible to retrieve the quaternions $\boldsymbol{q}_{\text{ADCS}} = [q_1; q_2; q_3; q_4] = [\boldsymbol{\varrho}; q_4]$ representing the CubeSat's attitude, by integrating the satellite kinematics of Equation 2:

$$\dot{\boldsymbol{q}}(t) = \frac{1}{2} \begin{bmatrix} 0 & \omega_z & -\omega_y & \omega_x \\ -\omega_z & 0 & \omega_x & \omega_y \\ \omega_y & -\omega_x & 0 & \omega_z \\ -\omega_x & -\omega_y & -\omega_z & 0 \end{bmatrix} \boldsymbol{q} \tag{2}$$

where the first three components of the quaternion vector constitute the vector part of the quaternions $\boldsymbol{\varrho}$, while the last element q_4 is the scalar part used for the normalization.[9]

From the quaternions, the direct cosine matrix representation (DCM) can be computed:[8] here $A_{B/N}$ is defined as the relative orientation between the body frame B and the inertial frame N and its behavior in time is described by a system of differential equations represented by:

$$\dot{A_{B/N}}(t) = - \begin{bmatrix} 0 & -\omega_3 & \omega_2 \\ \omega_3 & 0 & -\omega_1 \\ -\omega_2 & \omega_1 & 0 \end{bmatrix} A_{B/N}(t). \tag{3}$$

Afterward, estimates of the actual spacecraft attitude are derived through the attitude determination process: the measurements from the sensors are exploited to compute the actual rotational matrix $A_{B/N}$ by applying the singular value decomposition method to solve Wahba's problem.[8]

With regard to the desired attitude, the satellite baseline is implemented as Earth-pointing: in future developments, the opposite terminal or the OGS can be implemented as moving targets to simulate ISL and DTE. Therefore, assuming the chosen orbit and the positioning of LCT on the satellite bus, the ideal attitude is given by the rotation matrix from inertial to LVLH reference frame $A_{L/N}$, with the spacecraft's body reference frame aligned with the LVLH one to point the LCT toward the center of the Earth. As a result, the three-dimensional pointing errors $\boldsymbol{\varepsilon}_{\text{ADCS}}$ between the actual orientation of the satellite and the desired one are computed in the satellite body frame.

In order to achieve the desired attitude, the actuators have to transfer a torque to the spacecraft or exchange a moment with it to allow it to perform maneuvers and compensate for disturbances' torques. Two control algorithms have been here implemented for the satellite ADCS to guarantee closed-loop stability. The B-dot proportional law, which consists of a simplified control that switches on/off the magnetorquers,[8] is employed to reduce the satellite angular velocity in presence of highly dynamic scenarios as the detumbling manoeuvre. Moreover, the reaction wheels are used to maintain the CubeSat close to the desired attitude during a more stable attitude scenario, according to the non-linear control law[8] of Equation 4,

$$\boldsymbol{u}_c = -k_1\, \boldsymbol{\omega}_e - k_2 \left(A_e^T - A_e\right)^V + \boldsymbol{\omega} \times I\boldsymbol{\omega} \tag{4}$$

where $\boldsymbol{u}_c$ is the command given to the actuators, I is the inertia matrix, $\boldsymbol{\omega}$ is the satellite angular velocity, A_e is the attitude error and $\boldsymbol{\omega}_e$ the corresponding angular velocity error. The gains have been chosen as $k_1 = 0.08$ and $k_2 = 0.0065$, with k_2 being proportional to the error between the current attitude matrix and the desired attitude, and k_1 being proportional to the difference between the current angular velocity and the desired one.

The outputs of the ADCS baseline model result in the satellite angular velocity $\boldsymbol{\omega}_{\text{ADCS}}$, the quaternion vector $\boldsymbol{q}_{\text{ADCS}}$ and the pointing errors $\boldsymbol{\varepsilon}_{\text{ADCS}}$ that can then be fed to the LCT to study its augmented attitude concept.

LCT's Sensors

The optical communication terminal of the OSIRIS payload works at 200 Hz and is equipped with the optical block, the sensors and the control unit where the estimation algorithms are implemented.

The sensors consist of an IAM-20380 MEMS gyroscope and a RM-3100 3-axis magnetometer. Both sensors have been implemented in SIMULINK by following the specifications of their data-sheets (Table 1) and are considered to be calibrated already.[7,10]

Table 1: IAM-20380 gyroscope and RM-3100 magnetometer data-sheets

Parameter	Value	Unit
Gyroscope sampling frequency	200	Hz
Gyroscope range	± 250	dps
Gyroscope sensitivity	131	LSB/dps
Gyroscope rate noise density	0.01	dps/$\sqrt{\text{Hz}}$
Magnetometer sampling frequency	200	Hz
Magnetometer range	± 800	μT
Magnetometer sensitivity	26	nT
Magnetometer gain	33	μT
Magnetometer noise	20	nT
Magnetometer noise density	1.2	nT/Hz

The gyroscope model takes as input the actual angular velocity of the CubeISL satellite and gives as output the measured angular velocity in discrete time.

In detail, the input is firstly passed to a second-order transfer function, with natural frequency of $2\pi \cdot 1000\,\text{rad/s}$ and damping ratio of $\sqrt{2}/2$. After that, white noise is added to the signal with a sample time of $t_{\text{gyro}} = 1/200\,\text{s}$ and a noise power equal to the square of the rate noise spectral density. Then, the signal is transformed from degree per second dps to counts using a scale factor block with a gain equal to the inverse of the sensitivity. A digital low pass filter LPF is then added to filter out high frequencies, represented as a S-domain transfer function with cut-off frequency of 177 Hz and damping ratio of $\sqrt{2}/2$. Finally, a limit on the range is imposed through a saturation block with a range of 2^{15}, to circumvent values bigger than 16 bit, and the output $\boldsymbol{\omega}_{\text{gyro}}$ is transformed from continuous to discrete by a zero-order hold block and rotated into the LCT frame.
The magnetometer's SIMULINK model takes as input the magnetic field in the inertial reference frame (built according to the IGRF model[11]) and gives as output the measured field in both, inertial and LCT frame. In particular, white noise is added to the signal with noise mean and noise density chosen according to Table 1. Then, a discrete state-space block and a zero-order hold block are used to obtain a linear discrete signal with sample time $t_{\text{mag}} = 1/200\,\text{s}$. A quantizer and a gain block are also added to the mode.. Finally, a saturation block allows to obtain limited output with maximum range of $\pm 800\,\mu\text{T}$. Hence, the obtained magnetic field in inertial frame $\boldsymbol{b}_{\text{N}}$ is fist rotated into the satellite body frame and then into the LCT frame by applying the attitude rotation matrices:

$$\boldsymbol{b}_{\text{LCT,magn}} = R_{\text{LCT}\leftarrow\text{B}}\,(A_{\text{B/N}}\,\boldsymbol{b}_{\text{N}}). \tag{5}$$

METHODS FOR THE ATTITUDE KNOWLEDGE AUGMENTATION

The attitude estimation process aims to obtain an accurate estimate of the LCT's attitude in between two successive updates from the satellite's ADCS. Assuming that the satellite's ADCS operates at 1 Hz while the LCT has a frequency of 200 Hz, the updates are received every 1 s by the terminal. In this occasion, the LCT resets its attitude knowledge, represented by the estimated quaternion vector $\hat{\boldsymbol{q}}$, to the value of the quaternion vector of the ADCS knowledge $\boldsymbol{q}_{\text{ADCS}}$. In the interval between one update and the following, the LCT exploits an estimation algorithm to keep the error drift bounded and consequently augment the terminal's attitude knowledge. The estimation strategies considered for this purpose are either simple discretization, linear extrapolation, quaternions' kinematic propagation and UnScented QUaternion Estimator (USQUE) Unscented Kalman Filter. While the linear extrapolation relies only on the attitude information given by the ADCS updates, the quaternions' kinematics propagation can either use only the ADCS quaternions or combining it with the LCT's sensors measurements consisting of the angular velocity $\boldsymbol{\omega}_{\text{gyro}}$ measured from the MEMS gyroscope. In addition, two versions of the USQUE Kalman Filter, built from the model of Crassidis and Markley,[12] have been analyzed. For both filters, the information coming from the LCT consists of the gyroscope's angular velocity $\boldsymbol{\omega}_{\text{gyro}}$ and the magnetic field $\boldsymbol{b}_{\text{magn}}$ measured by the magnetometer. The first version can be referred to as the classic USQUE filter and accounts for the gyroscope bias $\boldsymbol{\beta}$ and the attitude error in the state vector. On the contrary, the other version takes advantage of the attitude error and the angular velocity of the state, where the latter is propagated in time according to the explicit satellite's dynamics, and is therefore called UnScented QUaternion Estimator with Satellite Dynamics (USQUESD).

Discretization and Linear Extrapolation of the Attitude

As initial approach, the vector of the discretized quaternions $\hat{\boldsymbol{q}}_{\text{discr}}$ is derived from the satellite updates by extracting the components of $\boldsymbol{q}_{\text{ADCS}}$ at the ADCS sampling rate of 1 Hz and holding these values constant between one update and the following one. The discretized vector represents the attitude information that the LCT receives every second from the satellite ADCS itself without any further processing. Another basic estimation strategy consists of the computation of the estimated quaternion $\hat{\boldsymbol{q}}_{\text{extrap}}$ by linear extrapolation: $\hat{\boldsymbol{q}}_{\text{extrap}}$ is computed from the two previously computed quaternions with a step size of 0.005 s, according to the LCT's sampling rate of 200 Hz. Thus, the extrapolation is performed in between the ADCS updates and every 1 s the value of $\hat{\boldsymbol{q}}_{\text{extrap}}$ is reset to $\boldsymbol{q}_{\text{ADCS}}$.

Discrete-Time Integration of the Quaternions Kinematics

Instead of making use of pure mathematical relations as for the linear extrapolation, another possibility is to propagate the quaternions by discrete-time integration of their kinematics.
This proposed strategy exploits the angular velocity $\boldsymbol{\omega}_{\text{gyro}}$ measured by the LCT gyroscope to compute the derivative of the quaternion vector $\boldsymbol{q} = [\boldsymbol{\varrho}; q_4]$

according to the quaternions attitude kinematics:[8]

$$\dot{\boldsymbol{q}}(t) = \frac{1}{2}\,\Xi[\boldsymbol{q}(t)]\,\boldsymbol{\omega}_{\text{gyro}}(t) \tag{6}$$

where $I_{3\times3}$ is the identity matrix and the quaternions matrix $\Xi[\boldsymbol{q}(t)]$ is computed from the quaternions cross product $[\boldsymbol{\varrho}]_\times$ as[9]

$$\Xi[\boldsymbol{q}(t)] \equiv \begin{bmatrix} q_4 I_{3\times3} + [\boldsymbol{\varrho}]_\times \\ -\boldsymbol{\varrho}^T \end{bmatrix} \tag{7}$$

The derivative is then integrated in discrete-time in order to recover the estimated quaternion vector $\hat{\boldsymbol{q}}_{\text{prop}}$ at each integration step of 0.005 s, according to the LCT's sampling frequency. Additionally, a reset of the estimated quaternion $\hat{\boldsymbol{q}}_{\text{prop}}$ occurs periodically every second by updating it with the ADCS baseline's quaternions $\boldsymbol{q}_{\text{ADCS}}$ to bound the estimation error drift (Figure 5).

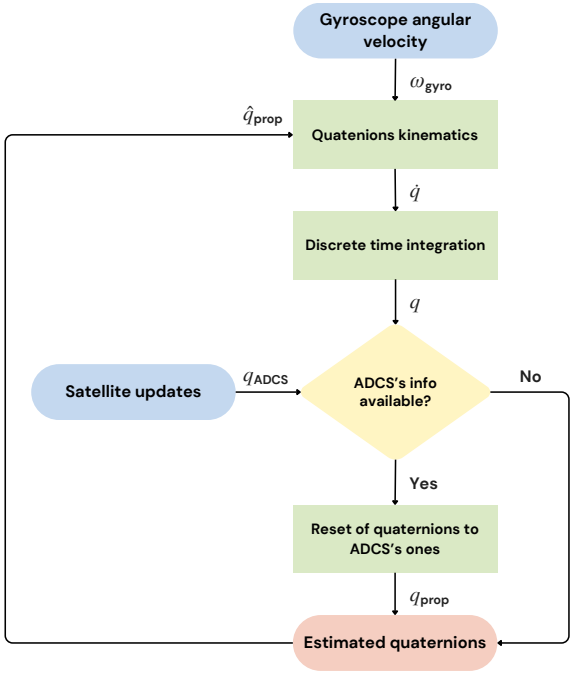

Figure 5: Concept of the discrete-time integration of the quaternions kinematics.

USQUE Kalman Filter

A more sophisticated algorithm for attitude estimation consists of the UnScented QUaternion Estimator USQUE, an unscented Kalman filter developed by Crassidis and Markley.[12]
The USQUE filter has been adopted instead of other dynamic filters based on the fact that it leads to low expected errors also for strong non-linearities of the models and a faster convergence from inaccurate initial conditions.[7,13] Moreover, it preserves the quaternion's normalization constraint at each step in the filter by exploiting a three-component multiplicative error quaternion $\delta\boldsymbol{p}$:

$$\delta\boldsymbol{p} = f\frac{\delta\boldsymbol{\varrho}}{a+\delta q_4} \tag{8}$$

where $\delta\boldsymbol{\varrho}$ and δq_4 are respectively the vectorial and scalar parts of the error $\delta\boldsymbol{q} = \boldsymbol{q}_{\text{ADCS}} \otimes \hat{\boldsymbol{q}}^{-1}$ between estimated $\hat{\boldsymbol{q}}$ and actual quaternions $\boldsymbol{q}_{\text{ADCS}}$ at each integration step. This local error quaternion consists of a generalized representation of the Modified Rodrigues Parameters where the filter's parameters have been taken as $a = 1$ and $f = 2(a+1) = 4$ to retrieve $\|\delta\boldsymbol{p}\|$ equal to the attitude estimation error $\boldsymbol{\vartheta}$ for small errors.[12]
The inverse transformations to find the scalar δq_4 and vectorial parts $\delta\boldsymbol{\varrho}$ of the error quaternion from $\delta\boldsymbol{p}$ are then given by:

$$\begin{aligned} \delta q_4 &= \frac{-a\|\delta\boldsymbol{p}\|^2 + f\sqrt{f^2 + (1-a^2)\,\|\delta\boldsymbol{p}\|^2}}{f^2 + \|\delta\boldsymbol{p}\|^2}, \\ \delta\boldsymbol{\varrho} &= f^{-1}(a+\delta q_4)\,\delta\boldsymbol{p}. \end{aligned} \tag{9}$$

The $\delta\boldsymbol{p}$ error is incorporated into the state vector of the system $\hat{\boldsymbol{x}}_{\text{USQUE}}$ along with the LCT gyroscope's bias $\boldsymbol{\beta}$, obtaining a $n = 6$ dimensional state associated with a 6×6 covariance matrix:

$$\hat{\boldsymbol{x}}_{\text{USQUE}} = \begin{bmatrix} \hat{\boldsymbol{\beta}} \\ \delta\hat{\boldsymbol{p}} \end{bmatrix}. \tag{10}$$

The gyroscope's bias $\boldsymbol{\beta}$ is derived from the model of the rate-integrating gyro according to Equation 11:

$$\begin{aligned} \boldsymbol{\omega}_{\text{gyro}}(t) &= \boldsymbol{\omega}_{\text{ADCS}}(t) + \boldsymbol{\beta}(t) + \boldsymbol{\eta}_v(t) \\ \dot{\boldsymbol{\beta}}(t) &= \boldsymbol{\eta}_u(t) \end{aligned} \tag{11}$$

with $\boldsymbol{\eta}_v(t)$ and $\boldsymbol{\eta}_u(t)$ as zero-mean Gaussian white-noises.
The filter's measurements are then constituted by the magnetic field vector measured by the LCT's magnetometer, according to the discrete-time attitude observations model of Equation 12.

$$\tilde{\boldsymbol{y}}_{\text{USQUE}} = A(\boldsymbol{q})\boldsymbol{r}_{\text{magn}} + \boldsymbol{v}_{\text{magn}}. \tag{12}$$

Considering the magnetometer as the only sensor, $\boldsymbol{r}_{\text{magn}} = \boldsymbol{b}_{\text{N}}$ is the reference vector representing the magnetic field in the inertial frame from the IGRF model,[11] $A(\boldsymbol{q})$ is the attitude matrix computed from the quaternions and $\boldsymbol{v}_{\text{magn}}$ is the Gaussian sensor error-vector of the magnetometer.

The initialization, prediction and update steps are then implemented according to Crassidis and Markley's model.[12] The output of the estimation process consists of the estimated quaternions $\hat{\boldsymbol{q}}_{\text{USQUE}}$ that can be retrieved from the $\delta\boldsymbol{p}$ part of the update state, with the reset to the updates $\boldsymbol{q}_{\text{ADCS}}$ every second, as shown in Figure 6.

USQUESD Filter with Satellite's Dynamics

The second version of the USQUE filter - Unscented QUaternion Estimator with Satellite's Dynamics (USQUESD) - overcomes again the problem of the quaternion's normalization by exploiting the local error quaternion $\delta\boldsymbol{p}$ as for the classical USQUE. In particular, the classical USQUE filter of Crassidis and Markley has been modified such that the state $\hat{\boldsymbol{x}}_{\text{USQUESD}}$ is composed by the CubeSat's attitude, represented by the local error quaternion $\delta\boldsymbol{p}$, and by the satellite's angular velocity $\boldsymbol{\omega}$[14,15] according to the state estimator model of the Spacecraft Dual Unscented Kalman Filter (SDUKF) of VanDyke, Schwartz, and Hall:[16]

$$\hat{\boldsymbol{x}}_{\text{USQUESD}} = \begin{bmatrix} \hat{\boldsymbol{\omega}} \\ \delta\hat{\boldsymbol{p}} \end{bmatrix}. \tag{13}$$

The state model follows Equation 8 for what concerns the attitude part $\delta\boldsymbol{p}$, while the angular velocity is found by integrating Euler's equations:

$$\begin{cases} I_x\dot{\omega}_x + (I_z - I_y)\,\omega_z\omega_y = M_x \\ I_y\dot{\omega}_y + (I_x - I_z)\,\omega_x\omega_z = M_y \\ I_z\dot{\omega}_z + (I_y - I_x)\,\omega_y\omega_x = M_z \end{cases} \tag{14}$$

The diagonal components of the inertia matrix I_x, I_y and I_z are considered fixed in time and equal to the ones of the satellite's baseline model. The total torque $M = [M_x;\, M_y;\, M_z]$ is instead given in real-time by the sum of the disturbances' and actuators' torques of the satellite model.
The set of measurements consists of the LCT's gyroscope angular velocity $\boldsymbol{\omega}_{\text{gyro}}$ and the magnetic field $\boldsymbol{b}_{\text{magn}}$ measured by the LCT's magnetometer according to the discrete-time observations model of Equation 15.

$$\tilde{\boldsymbol{y}}_{\text{USQUESD}} = \begin{bmatrix} \boldsymbol{\omega}_{\text{gyro}} \\ A(\boldsymbol{q})\boldsymbol{r}_{\text{magn}} \end{bmatrix} + \begin{bmatrix} \boldsymbol{\nu}_{\text{gyro}} \\ \boldsymbol{\nu}_{\text{magn}} \end{bmatrix}. \tag{15}$$

Again, the implementation of the filter follows the steps of the UKF algorithm of Crassidis and Markley[12] with a step size of 0.005 s and initialization, prediction and update steps based on the state estimation methodology of the SDUKF filter.[16] Indeed, the reset of the estimated quaternions $\hat{\boldsymbol{q}}_{\text{USQUESD}}$ is performed every 1 s (Figure 6).

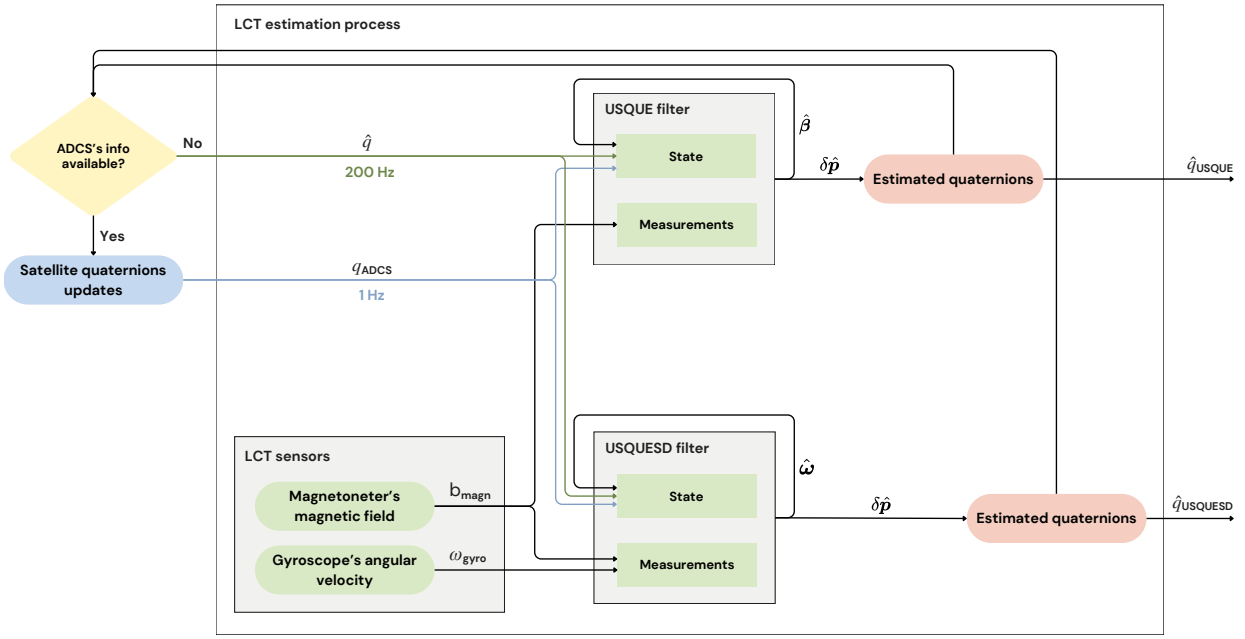

Figure 6: Block diagram of the estimation processes for the USCQUE and USQUESD filters.

IMPLEMENTATION AND RESULTS OF THE ESTIMATION ALGORITHMS

The estimation concept has been implemented in the SIMULINK environment to analyze and compare the performances of the proposed algorithms. Thus, two different mission scenarios have been simulated: a tumbling motion - here referred as dynamic attitude regime - and a more stable attitude motion - so-called nominal or stable attitude regime. This choice has been made to study the estimation performances for two different situations that can be representative of acquisition and tracking phases.
Indeed, the aim is to evaluate for both regimes, the improvement achieved by exploiting the additional attitude information from the LCT at 200 Hz compared to consider only the attitude updates received from the satellite at 1 Hz.

Simulating the Scenarios of the CubeISL's Baseline and LCT's Sensors Measurements

The results of CubeISL's baseline simulation are here presented for the dynamic and nominal regimes, with a desired attitude corresponding to the LCT's laser beam pointing toward the center of the Earth. The dynamic regime is assumed to represent a dynamic maneuver where the CubeSat is rotating in space, in a sort of slew/detumbling maneuver, to reach the desired orientation where it points toward the opposite target to establish a link. This scenario is here supposed to be characterized by an initial angular velocity $\boldsymbol{\omega}_{\text{ADCS},0} = [0.22; 0.24; 0.24]\,\text{rad/s}$ and angular accelerations bigger than $\pm 0.023\,\text{deg}\,\text{s}^{-2}$. The nominal regime instead is conceived as a more stable attitude around the desired orientation, where the satellite is slightly tumbling in proximity to the desired equilibrium orientation seeking the opposite target in the attempt of establishing or maintaining a link. In this situation the CubeSat exhibits peak angular accelerations of $\pm 0.023\,\text{deg}\,\text{s}^{-2}$ and an initial angular velocity $\boldsymbol{\omega}_{\text{ADCS},0} = [0.01; 0.01; 0.01]\,\text{rad/s}$. For both the simulations, an initial condition on the quaternion vector $\boldsymbol{q}_{ADCS,0} = [0; 0; 0; 1]$ and a simulation sampling rate of $10^{-4}\,\text{s}$ have been selected. From the obtained attitude quantities, the satellite updates are then fed to the LCT model for estimation purposes.
Figures 7 and 8 show an overview of the attitude outputs of the CubeISL satellite model, consisting of the satellite's angular velocity $\boldsymbol{\omega}_{\text{ADCS}}$ and quaternions $\boldsymbol{q}_{\text{ADCS}}$ for simulations of 800 s for the two considered regimes.

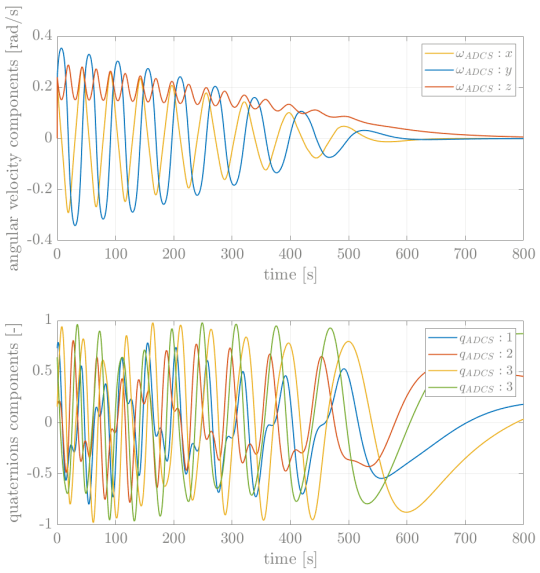

Figure 7: Simulation of the CubeISL baseline's angular velocity and quaternions for the dynamic regime.

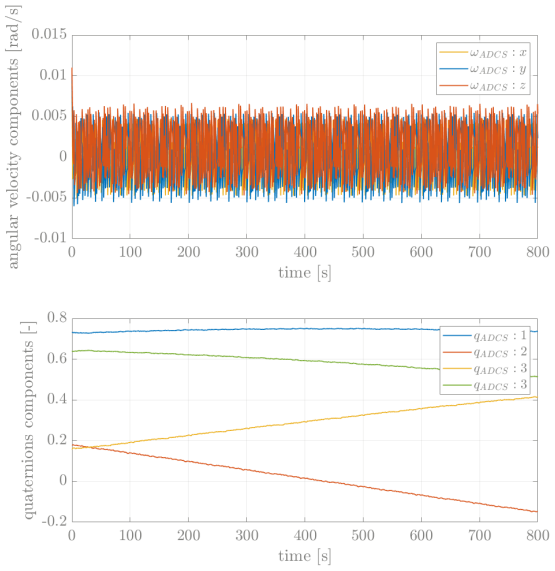

Figure 8: Simulation of the CubeISL baseline's angular velocity and quaternions for the nominal regime.

For the dynamics regime, it's possible to state that the baseline ADCS model well simulates the plausible behavior of a satellite's attitude in presence of rotations aimed to both point it toward a desired target and stabilize its attitude progressively. In this work, this situation has been simulated as a sort of detumbling manoeuvre where the angular velocity components reach an absolute value lower than

10^{-2} rad/s after about 800 s. In addition, the quaternions progressively damp their oscillations toward a desired almost constant behavior as can be observed in Figure 7.

From the nominal regime simulation, instead, the baseline's close-loop demonstrates the ability of granting attitude stability with an angular velocity that slightly oscillates around the desired equilibrium value ~ 0 rad/s. These oscillations around the respective nominal values are due mainly to environmental disturbances, imperfections in the control actions and non-ideality of the actuators that simulates the physical behavior of the CubeISL satellite in a plausible real-world scenario. Indeed, the simulated satellite quaternions $\boldsymbol{q}_{ADCS}$ follow the behaviour of the desired ones, computed from the desired attitude matrix A_{d}, as expected (Figure 8).

A relevant performance parameter for the baseline model in the nominal regime is its attitude accuracy, that can be represented as the pointing errors along the body axes directions $\boldsymbol{\varepsilon}_{3\mathrm{D}} = [\alpha_x, \alpha_y, \alpha_z]$ computed between the desired attitude (in presence of the miss-pointing command) and the CubeSat model's actual attitude[7] according to:

$$\tilde{A} = A_{\mathrm{B/N}}\, A_{\mathrm{d}}^{T} = \begin{bmatrix} 1 & \alpha_z & -\alpha_y \\ -\alpha_z & 1 & \alpha_x \\ \alpha_y & -\alpha_x & 1 \end{bmatrix} \tag{16}$$

where A_{d} corresponds to the rotation between the inertial frame and the satellite body frame for the desired LVLH-pointing. From simulations, it has been found that the Root Mean Squared Errors (RMSE) over time for the $\boldsymbol{\varepsilon}_{3\mathrm{D}}$ errors result in $\mathrm{RMSE}_{\varepsilon} = [0.091, 0.088, 0.101]$ deg. These errors prove a really good accuracy of the ADCS closed-loop that satisfy the mission requirements on the pointing accuracy of the satellite platform - that should present pointing errors lower than ± 1 deg.

From simulations, the gyroscope model demonstrated to be able to measure the actual value of the satellite's angular velocity with the addition of noise, due to the physical sensor itself. In particular, this noise resulted to be lower than ± 0.45 deg/s, proving a correct implementation of the gyroscope model. Moreover, the magnetometer model produced a measured magnetic field vector that well represented the behavior of the reference magnetic field in inertial and body-frame with an intrinsic added noise of the order of 2 µT.

Convergence Study for the Kalman Filters

A preliminary analysis has been conducted on the convergence of the two USQUE filters without applying the reset of the estimated quaternions to the ADCS updates. This study has been made in order to assess the filter convergence in time without forcing their output to the ADCS reference one every 1 s. Two simulations have been conducted for both filters considering respectively a reference attitude in presence of fast dynamic manoeuvre (dynamic regime) or a stable attitude in proximity of the equilibrium orientation (nominal regime). Therefore, the outputs of the satellite baseline model - quaternions $\boldsymbol{q}_{\mathrm{ADCS}}$ and angular velocity $\boldsymbol{\omega}_{\mathrm{ADCS}}$ - and of the LCT sensors models - gyroscope's angular velocity $\boldsymbol{\omega}_{\mathrm{gyro}}$ and magnetometer's measured magnetic field $\boldsymbol{b}_{\mathrm{magn}}$ - have been exploited as inputs to the filters to perform the attitude estimation.

The initial conditions for the simulations are shown in Table 2 for the two filters respectively.

Table 2: Tuning and initial parameters for the USQUE and USQUESD filters

Parameter	USQUE	USQUESD
β_0	0.1 deg/h	-
$\omega_{0,dyn}$	-	0.2 rad/s
$\omega_{0,nom}$	-	0.01 rad/s
$\delta\boldsymbol{p}_0$	[0;0;0]	[0;0;0]
$\boldsymbol{q}_0$	[0;0;0;1]	[0;0;0;1]
$\sigma_{\beta,dyn}$	1 deg	-
$\sigma_{\beta,nom}$	0.1 deg/h	-
$\sigma_{\omega,dyn}$	-	10 deg
$\sigma_{\omega,nom}$	-	1 deg
$\sigma_{\delta\boldsymbol{p},dyn}$	50 deg	50 deg
$\sigma_{\delta\boldsymbol{p},nom}$	1 deg	1 deg
$\sigma_{Q,\omega}$	-	0.05 deg/s
$\sigma_{Q,\delta\boldsymbol{p}}$	-	$1{\cdot}10^{-9}$ rad
ARW_{noise}	0.1 deg/h/$\sqrt{Hz}$	-
BRW_{β}	0.01 deg/h	-
B_{gyro}	200 Hz	-
$t_{bias,gyro}$	1 h	-
σ_{gyro}	-	0.01 deg/s/$\sqrt{Hz}$
σ_{magn}	0.2 μT	0.2 μT

From the USQUE's values, the initial state can be retrieved as $\hat{\boldsymbol{x}}_{\mathrm{USQUE},0} = [\boldsymbol{\beta}_0;\, \delta\boldsymbol{p}_0]$ where the local quaternion error is initialized to zero and the bias of the gyroscope to 0.1 deg/h.[12] The initial covariance matrix $P_{\mathrm{USQUE},0}$ is built from initial values of σ_{β} for the gyroscope bias and $\sigma_{\delta\boldsymbol{p}}$ for the local error quaternion (for dynamic and nominal regimes) as:

$$P_{\mathrm{USQUE},0} = \begin{bmatrix} \sigma_{\beta}^2\, \mathbf{1}_{3\times 3} & 0_{3\times 3} \\ 0_{3\times 3} & \sigma_{\delta\boldsymbol{p}}^2\, \mathbf{1}_{3\times 3} \end{bmatrix}. \tag{17}$$

The process noise matrix $\bar{Q}_{\text{USQUE}}$ can be computed starting from the typical values of an angular random walk ARW_{gyro}, a bias random walk BRW_β ,[17] a gyroscope's bandwidth B_{gyro}[18] and a bias instability's time parameter $t_{bias,gyro}$[19] (Table 2). It is indeed possible to retrieve the standard deviation related to the gyroscope angular random noise $\sigma_v = 2.0569 \cdot 10^{-6}\,\text{rad/s}^{1/2}$ and the one linked to the drift rate $\sigma_u = 4.6651 \cdot 10^{-10}\,\text{rad/s}^{3/2}$ (Equation 18).

$$\begin{aligned} \sigma_v &= ARW_{gyro}\sqrt{B_{gyro}} \\ \sigma_u &= BRW_\beta / \sqrt{3 \cdot t_{bias,gyro}} \end{aligned} \tag{18}$$

These quantities can be combined with the sampling interval of the LCT's gyroscope $\Delta t = 0.005\,\text{s}$ to compute the $\bar{Q}_{\text{USQUE}}$ matrix as:

$$\bar{Q} = \frac{\Delta t}{2} \begin{bmatrix} \sigma_u^2 \mathbf{1}_{3\times3} & 0_{3\times3} \\ 0_{3\times3} & \left(\sigma_v^2 - \frac{1}{6}\sigma_u^2 \Delta t^2\right) \mathbf{1}_{3\times3} \end{bmatrix}. \tag{19}$$

Additionally, the observation model's noise matrix R_{USQUE} can be computed from the magnetometer accuracy according to:

$$R_{\text{USQUE}} = \sigma_{\text{magn}}^2\, \mathbf{1}_{3\times3}. \tag{20}$$

Similarly, the USQUESD initial values of Table 2 are used to compute the initial state $\hat{\boldsymbol{x}}_{\text{USQUESD},0} = [\boldsymbol{\omega}_0;\, \delta\boldsymbol{p}_0]$, with the local quaternion error initialized to zero and the initial angular velocity components to $\omega_{0,dyn}$ and $\omega_{0,nom}$ for the two simulation scenarios, respectively. The initial covariance matrix $P_{\text{USQUESD},0}$ is computed from the initial standard deviations:

$$P_{\text{USQUESD},0} = \begin{bmatrix} \sigma_\omega^2\, \mathbf{1}_{3\times3} & 0_{3\times3} \\ 0_{3\times3} & \sigma_{\delta\boldsymbol{p}}^2\, \mathbf{1}_{3\times3} \end{bmatrix}. \tag{21}$$

The process noise matrix Q_{USQUESD} includes three-diagonal elements related to the angular velocity - and due to torque noises induced by the satellite's actuators - and three other elements related to the local error quaternion. For both dynamic and nominal regimes, it can be computed as:

$$Q_{\text{USQUESD}} = \begin{bmatrix} \sigma_{Q,\omega}^2 \mathbf{1}_{3\times3} & 0_{3\times3} \\ 0_{3\times3} & \sigma_{Q,\delta p}^2 \mathbf{1}_{3\times3} \end{bmatrix}. \tag{22}$$

The observations noise matrix R_{USQUESD} is found from the LCT's gyroscope and magnetometer accuracies:

$$R_{\text{USQUESD}} = \begin{bmatrix} \sigma_{\text{gyro}}^2\, \mathbf{1}_{3\times3} & 0_{3\times3} \\ 0_{3\times3} & \sigma_{\text{magn}}^2\, \mathbf{1}_{3\times3} \end{bmatrix}. \tag{23}$$

The simulations have been carried out for 800 s for the two filters exploiting the attitude reference of the satellite baseline and LCT sensors models for the dynamic and nominal regimes. Figure 9 shows the comparison between the satellite quaternions $\boldsymbol{q}_{\text{ADCS}}$ and the quaternions estimated by the USQUE filter $\hat{\boldsymbol{q}}_{\text{USQUE}}$: for both dynamic and nominal regimes, the estimated quantities well represent the real attitude ones, demonstrating a fast convergence capability after an interval of about 140 s for the nominal scenario and after only 50 s for the dynamics one. Thus, a good estimation result is maintained for the whole simulation time.

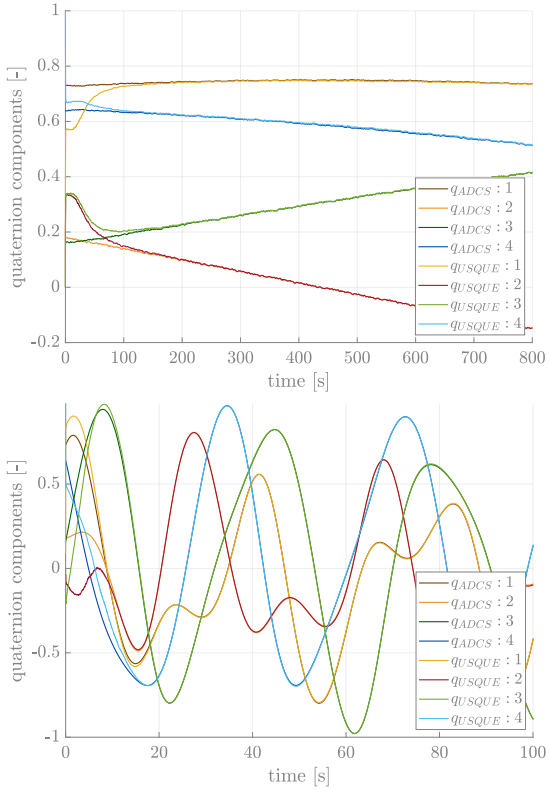

Figure 9: Convergence of the USQUE's estimated quaternions to the satellite's quaternions for the nominal (above) and dynamic (below) regimes.

Similar considerations are valid for the USQUESD, that reached convergence after about 160 s for the nominal and again 50 s for the dynamic regime. In addition, both filters are estimating correctly the gyroscope bias, giving a consequently corrected estimation of the angular velocity. The convergence of the filters in presence of both small -nominal regime- and bigger initial attitude errors -dynamic regime- is proven also by the fact that the square roots of the traces of the two diagonal sub-matrices of P_{USQUE} and P_{USQUESD} get smaller with time along the considered interval. An example is shown in Figure 10,

for the simulation of the USQUE in the nominal regime: the dispersion from the mean state at each epoch diminishes with the passage of time for both bias and quaternion error parts, reaching a minor discrepancy from the mean at the final epoch.

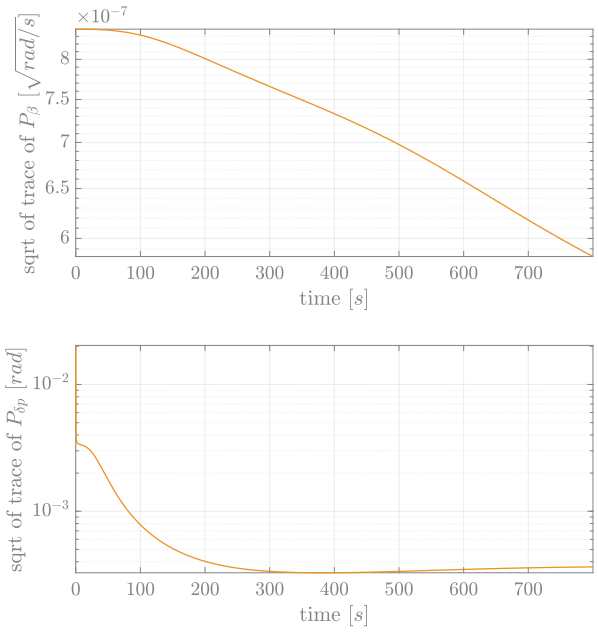

Figure 10: Square roots of the traces of USQUE sub-covariances for the nominal regime (semi-logarithmic scale).

Since both the filters are characterized by the parameters $a = 1$ and $f = 2(a + 1)$ and subjected to small errors, the attitude error can be here approximated as the norm of the updated local error quaternion $\delta\boldsymbol{p}$ before its reset to zero at the end of each iteration of the filters, according to the definition of the generalized Modified Rodrigues Parameters:[12]

$$\vartheta_{\delta\boldsymbol{p}} = \|\delta\boldsymbol{p}\| \,. \tag{24}$$

Indeed, the RMSE of this normalized attitude error $\vartheta_{\delta\boldsymbol{p}}$ has been computed for the two filters in the two considered regimes after 200 s (thus after the filters reached convergence) for the USQUE and USQUESD. The results presented in Table 3 show that the filters estimate the satellite quaternions with accurate precision and maintain the convergence for the whole simulation time.

Table 3: RMSE of the error $\vartheta_{\delta\boldsymbol{p}}$ before the reset step of the filters

Algorithm	Dynamic regime	Nominal regime
USQUE	2.0583 $\cdot 10^{-4}$ deg	1.1239 $\cdot 10^{-4}$ deg
USQUESD	1.8022 $\cdot 10^{-3}$ deg	1.8698 $\cdot 10^{-3}$ deg

Thus, the USQUE filter can be considered overall better in terms of pointing accuracy reached, while the time required for the filter to converge is similar with respect to the USQUESD version.
In addition, the computational times of the codes of the two filters have been computed with the Tic-Toc command in the MATLAB environment, by feeding them the previous-stored attitude quantities coming from the baseline model and LCT sensors. The measurements have been repeated for 100 iterations of 800 s on the same computer, and the mean of the obtained values has been found for the scenarios: the computational times for the USQUESD are one order of magnitude bigger than the ones of the USQUE ($\sim$ 300 s against $\sim$ 20 s) for both regimes. This shows that the USQUESD leads to a heavier computational burden for the on-board processor of the LCT due to the additional integration of the Euler dynamic equations at each epoch, that are not present in the classical USQUE.
As a final remark, it can be noted that multiple studies have been carried out on Kalman Filters for spacecraft attitude estimation employing a gyro and a 3-axes magnetometer, as for the USQUE. Specifically, it has been demonstrated[20] that these filters work for satellites operating at low altitudes in inclined orbits, where a good approximation of the Earth's magnetic field and sufficient observability of the attitude around all three axes is available. Nevertheless, a lack of observability due to a constant value of magnetic field reference can be experienced in lab-tests: this scenario is different from the real one where the satellite orbits through different zones of the Earth's magnetic field, but has to be considered as a possible explanation of the filters during hardware testing with microcontroller firmware in the laboratory in absence of a Helmholtz cage.[21] Possible solutions to this issue can be found by exploiting the derivative of the magnetic field as an additional measurement[15] or by augmenting the system state with local error quaternion, gyroscope bias and angular velocity in a sort of combined USQUE+USQUESD filter.[22] However, both solutions increase complexity of the models and a consequent increase of the computational time and effort for the on-board processor of the LCT.

Simulation and Analysis of the Attitude Estimation Methods

All the proposed algorithms have been implemented in a SIMULINK environment and their estimation has been tested for simulations over 800 s for the dynamic and static regimes.

The direct use of the satellite's attitude updates, here referred as the discretization method, does not estimate the quaternion values between successive updates, but keeps instead the same value for the whole interval of 1 s. Nevertheless, it is important to assess its performance as it represents the simplest form of using the ADCS attitude knowledge and is used as a baseline to evaluate the improvements by the proposed alternatives.
To quantify the accuracy reached by each algorithm, the respective pointing error quaternions $\boldsymbol{q}_{err}$ are computed for all the algorithms by subtracting the estimated quaternions $\hat{\boldsymbol{q}}$ ($\hat{\boldsymbol{q}}_{\text{discr}}$, $\hat{\boldsymbol{q}}_{\text{extrap}}$, $\hat{\boldsymbol{q}}_{\text{prop}}$, $\hat{\boldsymbol{q}}_{\text{USQUE}}$ and $\hat{\boldsymbol{q}}_{\text{USQUESD}}$) from the actual ones:[8]

$$\boldsymbol{q}_{err} = \hat{\boldsymbol{q}} - \boldsymbol{q}_{\text{ADCS}}. \tag{25}$$

Moreover, the error ϑ_{vect} is computed on the vectorial part $\delta\boldsymbol{\varrho}$ of the error quaternion $\delta\boldsymbol{q}$ between estimated $\hat{\boldsymbol{q}}$ and actual ADCS baseline's quaternions $\boldsymbol{q}_{\text{ADCS}}$ at each epoch:

$$\vartheta_{\text{vect}} = 2\arcsin\|\delta\boldsymbol{\varrho}\|. \tag{26}$$

Figures 11 and 12 show the behavior of ϑ_{vect} for the proposed algorithms in the nominal and dynamic regimes.

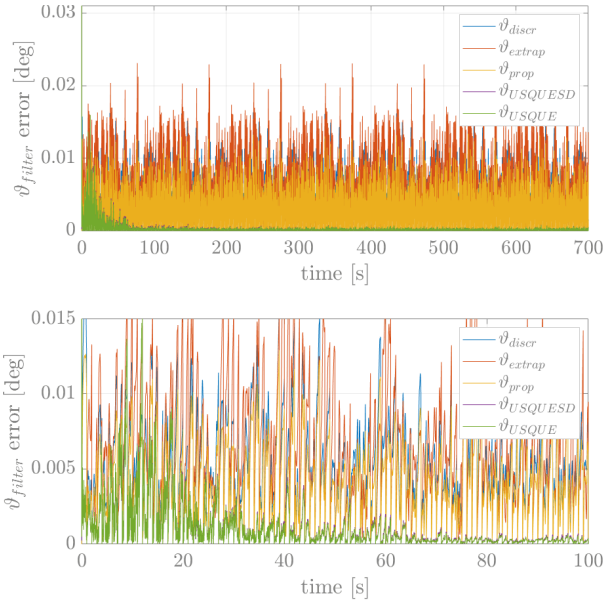

Figure 11: Comparison of ϑ_{vect} errors for the nominal regime (zoom in the plot below).

For the nominal scenario, the discretization, linear extrapolation and quaternion propagation show an almost constant trend over time, with the corresponding errors ϑ_{discr}, $\vartheta_{\text{extrap}}$ and ϑ_{prop} exhibiting similar absolute values over the simulation epochs. This can be explained by the fact that in this scenario the reference attitude changes gradually enough to not acquire critically large errors between ADCS updates. Therefore, it can be estimated decently well even by simple discretization or linear extrapolation. The quaternion propagation, instead, leverages the LCT information, yielding sligthly reduced errors in comparison to discretization and linear extrapolation, but is not able to reach the accuracy given by the USQUE and USQUESD. This is due to the fact that this method is hindered by the presence of noise, which affects the estimation through integration from the MEMS gyroscope measurements and limits the minimum attainable estimation error. The most significant improvements in the estimation results are exhibited by the filters, which overcome this limitation due to the unscented estimation filtering, with the errors ϑ_{USQUE} and $\vartheta_{\text{USQUESD}}$ being one order of magnitude smaller" with respect to the ones of the other algorithms. This is valid not only after the filters have already reached convergence but also during the first intervals of the simulation. The plot over the first one hundred seconds shows that the estimation errors for both filters decrease in absolute value in the initial epoch's of the simulation, in a sort of convergence that takes advantage of the previous epoch information even when the reset to the updates is applied. After the converge is reached, ϑ_{USQUE} and $\vartheta_{\text{USQUESD}}$ stabilize around a constant value.
In the dynamic regime, instead, the difference in estimation achieved by the different algorithms is more marked, as shown in Figure 12.

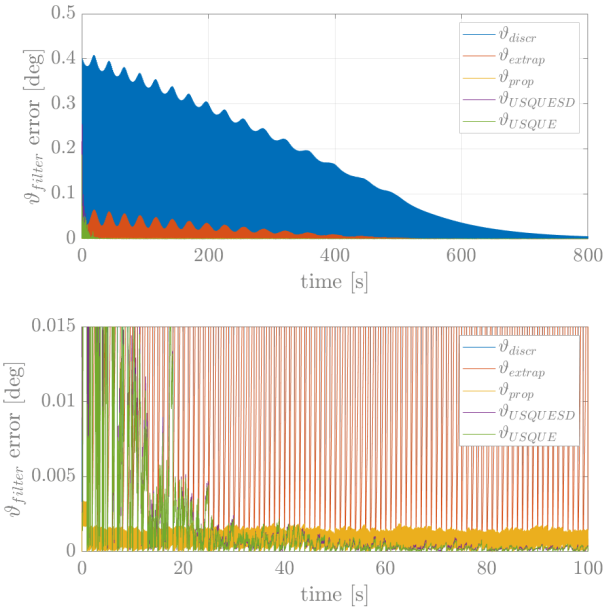

Figure 12: Comparison of ϑ_{vect} errors for the dynamic regime (zoom in the plot below).

Again, it can be observed that the filters yield superior performance, with ϑ_{USQUE} and $\vartheta_{\text{USQUESD}}$ exhibiting a significantly lower magnitude with respect to the other methods. This can be attributed to the fact that, in scenarios where attitudes undergo rapid and substantial changes, a linear function for extrapolation is inadequate due to the non-linear dynamics of the quantities being estimated. Moreover, the rapid fluctuations in the angular rate result in substantial variations in the attitude between successive updates: the algorithms that do not exploit the LCT - discretization and linear extrapolation - are unable to adequately capture these trajectories due to the limited sampling rate which is orders of magnitude slower than the changes in the attitude. Again, the quaternion propagation exhibits smaller errors in comparison to discretization and linear extrapolation, but it's estimation accuracy is limited by the noise of the gyroscope measurements.

To have a quantitative comparison between the proposed algorithms, the RMSE of the quaternion errors and on the vectorial errors is computed over the simulation times (excluding an initial converge time of 200 s for the filters). Subsequently, the vectorial norm of the obtained RMSE is taken for the quaternion error, reading $\|\text{RMSE}_{\boldsymbol{q}_{err}}\|$. Table 4 shows the computed results for all the methods and all the scenarios. These results confirm the observations already discussed: the two Kalman filters perform overall better with respect to the other proposed methods, with $\|\text{RMSE}_{\boldsymbol{q}_{err}}\|$ and $\text{RMSE}_{\vartheta_{vect}}$ being at least one order of magnitude smaller for both the regimes. Considering the two filters, the USQUE shows slightly superior performance than the USQUESD in terms of the estimation errors of Table 4. Given that the classical USQUE leads to a more accurate estimation, while requiring a convergence time comparable to the USQUESD and a significant smaller computational time, this filter is overall preferred for the analyzed scenario of the CubeISL mission.

To conclude, from the obtained results, it's clear that the presence of any estimation performed by the LCT leads to an improvement in the attitude knowledge between the updates of the satellite's attitude. This is especially true when comparing the use of the LCT - quaternions propagation and filters - to using only the ADCS's updates information - represented by the discretization method. By focusing on the USQUE algorithm, the achieved ϑ_{USQUE} amounts to respectively 3.63% and 0.17% of the discretized original error for the nominal and dynamic regimes , according to:

$$\%\,\vartheta = \frac{\text{RMSE}_{\vartheta_{USQUE}}}{\text{RMSE}_{\vartheta_{discr}}} \times 100. \tag{27}$$

Thus, with this approach the residual errors are reduced by a factor of over 27.5 in the nominal and 580 in the dynamic regime, enabling a significant improvement of the optical link acquisition and stability and, hence, data transmission reliability.

CONCLUSIONS

This work emphasized on improving the accuracy of the attitude estimation available to CubeSats hosting LCTs. This was achieved by exploiting the additional attitude information from the LCT itself instead of only relying on the attitude updates received periodically from the satellite.

To achieve this, different algorithms for attitude estimation have been studied, including linear extrapolation and quaternions propagation. It has been shown by simulations, that a dedicated Kalman filter can be implemented on the LCT's micro-processor to make use of the local attitude sensors, providing faster but less precise measurements, and of the slower but more accurate updates of the satellite's ADCS. Since this method relies on propagating a relative error with respect to the satellite output, two variants of an USQUE algorithm have been implemented and tested. Both variants showed better performance compared to the other methods and reached an attitude accuracy that is well within the requirements for the reference scenario of the

Table 4: Performance parameters of the estimation algorithms for the two regimes

	$\|\mathbf{RMSE}_{\boldsymbol{q}_{err}}\|$, -		$\mathbf{RMSE}_{\boldsymbol{\vartheta}_{\text{vect}}}$, deg	
Algorithm	**Dynamic regime**	**Nominal regime**	**Dynamic regime**	**Nominal regime**
Discretization	$6.2262 \cdot 10^{-2}$	$3.0998 \cdot 10^{-3}$	7.1392	0.3552
Linear extrapolation	$1.0161 \cdot 10^{-2}$	$3.9099 \cdot 10^{-3}$	0.6264	0.4480
Quaternion propagation	$2.9049 \cdot 10^{-4}$	$2.4878 \cdot 10^{-3}$	0.0332	0.2850
USQUE filter	$1.0634 \cdot 10^{-4}$	$1.1239 \cdot 10^{-4}$	0.0123	0.0129
USQUESD filter	$1.0820 \cdot 10^{-4}$	$1.1460 \cdot 10^{-4}$	0.0124	0.0131

CubeISL mission. It was demonstrated that the classical USQUE filter, led to estimation errors more than 500 times smaller compared to not using any LCT measurements and relying only on the satellite's information. Indeed, this approach can significantly reduce acquisition times and, consequently, improve the chance of a successful link. Furthermore, once a successful link has been established, a longer time window is available for the transmission of crucial payload data.
In future developments, the augmented attitude information could be passed to the FSM of the LCT and be then used to compensate for bigger pointing errors in a feed-forward manner. Moreover, the pointing error measured by the LCT's 4-quadrant diode during a link, could be given as a feedback to the satellite's estimation system to further improve the platform's pointing during the tracking phase of the mission.

ACKNOWLEDGEMENTS

The Authors would like to thank the entire CubeISL team at the German Aerospace Center.
This research work is supported by the German Federal Ministry of Defense through the technological research and development assignment "Responsive Space Capabilities".

References

[1] Christopher Schmidt and Christian Fuchs. The osiris program—first results and outlook. In *2017 IEEE International Conference on Space Optical Systems and Applications (ICSOS)*, pages 19–22. IEEE, 2017.

[2] Siegfried Janson and Richard Welle. The nasa optical communication and sensor demonstration program. 2013.

[3] Jessica Chang, CM Schieler, KM Riesing, JW Burnside, K Aquino, and BS Robinson. Body pointing, acquisition and tracking for small satellite laser communication. In *Free-Space Laser Communications XXXI*, volume 10910, pages 144–152. SPIE, 2019.

[4] Benjamin Rödiger, Rene Rüddenklau, Christopher Schmidt, and Marc Lehmann. Acquisition concept for inter-satellite communication terminals on cubesats. In *Small Satellites Systems and Services-The 4S Symposium 2022*, 2022.

[5] Jorge Rosano Nonay, René Rüddenklau, Andreas Sinn, Jan Paul Jakobs, Jonas Berlitz, Benjamin Rödiger, and Georg Schitter. Horizontal free-space optical link with cubeisl over 143 km. *Journal of Optical Communications and Networking*, 16(5):593, 2024.

[6] René Rüddenklau and Georg Schitter. Optimisation of acquisition patterns for establishing inter cubesat optical communications. *Journal of Optical Communications and Networking*, 2024.

[7] Elisa Garbagnati. Kalman filter based attitude estimation for cubesat missions in free-space optical communications. Master's thesis, Politecnico di Milano, 2021.

[8] F Landis Markley, John L Crassidis, F Landis Markley, and John L Crassidis. *Correction to: Fundamentals of Spacecraft Attitude Determination and Control*. Springer, 2014.

[9] Malcolm D Shuster et al. A survey of attitude representations. *Navigation*, 8(9):439–517, 1993.

[10] Simon Spier. Calibration of sensors for attitude determination on cubesats for optical inter-satellite links. Master's thesis, Technische Hochschule Mittelhessen, 2023.

[11] Arnaud Chulliat, William Brown, Patrick Alken, Ciaran Beggan, Manoj Nair, Grace Cox, Adam Woods, Susan Macmillan, Brian Meyer, and Michael Paniccia. The us/uk world magnetic model for 2020-2025: Technical report. 2020.

[12] John L Crassidis and F Landis Markley. Unscented filtering for spacecraft attitude estimation. *Journal of guidance, control, and dynamics*, 26(4):536–542, 2003.

[13] Fredrik Gustafsson and Gustaf Hendeby. Some relations between extended and unscented kalman filters. *IEEE Transactions on Signal Processing*, 60(2):545–555, 2011.

[14] Mohammad Abdelrahman and Sang-Young Park. Sigma-point kalman filtering for spacecraft attitude and rate estimation using magnetometer measurements. *IEEE Transactions on Aerospace and Electronic Systems*, 47(2):1401–1415, 2011.

[15] Sung-Woo Kim, Mohammad Abdelrahman, Sang-Young Park, and Kyu-Hong Choi. Unscented kalman filtering for spacecraft attitude and rate determination using magnetome-

ter. *Journal of Astronomy and Space Sciences*, 26(1):31–46, 2009.

[16] Matthew C VanDyke, Jana L Schwartz, Christopher D Hall, et al. Unscented kalman filtering for spacecraft attitude state and parameter estimation. *Advances in the Astronautical Sciences*, 118(1):217–228, 2004.

[17] Lubin Chang, Baiqing Hu, and Guobin Chang. Modified unscented quaternion estimator based on quaternion averaging. *Journal of Guidance, Control, and Dynamics*, 37(1):305–309, 2014.

[18] Marzio Agistri. Star tracker measurement filtering via uf/ekf with recursive prefiltering of imu reading. 2021.

[19] R Farrenkopf. Generalized results for precision attitude reference systems using gyros. In *Mechanics and Control of Flight Conference*, page 903, 1974.

[20] Mark L Psiaki, Francois Martel, and Parimal K Pal. Three-axis attitude determination via kalman filtering of magnetometer data. *Journal of Guidance, Control, and Dynamics*, 13(3):506–514, 1990.

[21] Salvatore Barone. *Numerical and Hardware-In-The-Loop Validation of an Attitude Estimation Algorithm for CubeSat Free-Space Optical Communication Terminals*. PhD thesis, Universita degli studi di Napoli Federico II, 2024.

[22] O-Jong Kim, Hanjoon Shim, Sunkyoung Yu, Yonghwan Bae, Changdon Kee, Hakdu Kim, Jungchul Lee, Jinhee Han, Sanghyuck Han, and Yeonju Choi. In-orbit results and attitude analysis of the snuglite cube-satellite. *Applied Sciences*, 10(7):2507, 2020.